Illumination Distribution from Brightness in Shadows: Adaptive Estimation of Illumination Distribution with Unknown Reflectance Properties in Shadow Regions

Imari Sato, Yoichi Sato, and Katsushi Ikeuchi
Institute of Industrial Science, University of Tokyo
7-22-1 Roppongi, Minato-ku, Tokyo 106-8558, Japan
{imarik, ysato, ki}@iis.u-tokyo.ac.jp

Abstract

This paper describes a new method for estimating the illumination distribution of a real scene from a radiance distribution inside shadows cast by an object in the scene. First, the illumination distribution of the scene is approximated by discrete sampling of an extended light source. Then the illumination distribution of the scene is estimated from a radiance distribution inside shadows cast by an object of known shape onto another object in the scene. Instead of assuming any particular reflectance properties of the surface inside the shadows, both the illumination distribution of the scene and the reflectance properties of the surface are estimated simultaneously, based on iterative optimization framework. In addition, this paper introduces an adaptive sampling of the illumination distribution of a scene. Rather than using a uniform discretization of the overall illumination distribution, we adaptively increase sampling directions of the illumination distribution based on the estimation at the previous iteration. Using the adaptive sampling framework, we are able to estimate overall illumination more efficiently by using fewer sampling directions. The proposed method is effective for estimating an illumination distribution even under a complex illumination environment.

1 Introduction

Image brightness is a function of shape, reflectance, and illumination [4]. The relationship among them has provided three major research areas in physics-based vision: shape-from-brightness (with a known reflectance and illumination) [6, 7, 8, 16], reflectance-from-brightness (with a known shape and illumination) [9, 1, 11, 12, 15, 17], and illumination-from-brightness (with a known shape and reflectance).

In the past, shape-from-brightness and reflectance-from-brightness have been extensively explored. In contrast, relatively limited amounts of research have been conducted in the third area, illumination-from-brightness [3, 14]. Some researchers attacked this problem as a related analysis of shape-from-shading. For example, Brooks and Horn determine shape as well as light sources from image brightness [7]. However, their analyses are conducted under very specific illumination conditions as in, for example, the case where there is only one direct light source in the scene; the analyses cannot be extended for more natural illumination conditions that include many types of direct and indirect illumination.

Recently, we proposed a method to recover an illumination distribution of a scene from image brightness with known shape and reflectance of an real object [19]. The method modeled illumination distribution of the scene with discrete sampling of the illumination radiance distribution, then formulated them as a simultaneous linear equation of unknown point sources. Then their brightness was determined by solving them from observed radiance changes inside shadows cast by an object of known shape onto another object surface of known shape and reflectance.[1] This method was effective and could estimate an illumination distribution even under a complex illumination environment such as an ordinary office, including reflections from the wall and other objects in the scene.

This method, however, has two limitations. First, it assumes that the reflectance properties of the surface inside shadows are given a priori. Otherwise, the method is applicable only if the surface is a Lambertian surface. Second, since the method uses a uniform discretization of the overall illumination for the estimation, the number of sampling

[1] In the past, shadows have been used for determining the 3D shapes and orientations of an object which cast shadows onto the scene [2, 10, 13, 20], while very few studies have focused on the the illumination information which shadows could provide.

0-7695-0164-8/99 $10.00 (c) 1999 IEEE

directions of illumination tends to be exceedingly large in order to accurately approximate the illumination distribution.

This paper presents a method to overcome these limitations. The solution consists of two main aspects. First, we combine the illumination analysis with an estimation of the reflectance properties of a surface inside shadows. As a consequence, the proposed method becomes applicable to the case where reflectance properties of a surface are not known. This enlarges the variety of images to which the method can be applied. Second, we propose an adaptive sampling framework for efficient estimation of illumination distribution. Rather than using a uniform discretization of the overall illumination distribution, we adaptively increase the sampling directions of the illumination distribution based on the estimation at the previous iteration. Using this adaptive sampling framework, we can avoid unnecessarily dense sampling of the illumination and estimate the entire illumination distribution more efficiently with a smaller number of sampling directions of the illumination distribution.

Our method estimates the illumination distribution of a real scene by using a single color image of the scene with shadows cast by an object. The rest of the paper refers to the image with shadows as the *shadow image*, to the object which casts shadows onto the scene as the *occluding object*, and to the surface onto which the *occluding object* casts shadows as the *shadow surface*. In our experiments, we recovered the camera parameters and the shape of the *occluding object* by using a photo-modeling tool interactively.[2]

The rest of the paper is organized as follows. We first obtain a formula which relates an illumination distribution of a scene with the image irradiance of the *shadow image* in Section 2. In Section 3, we describe the basic steps of the proposed method for simultaneously estimating both an illumination distribution of a scene and reflectance properties of the *shadow surface*. In Section 4, we explain how to estimate an illumination radiance distribution from given reflectance parameters of the *shadow surface* and the observed image irradiance of a *shadow image*. In Section 5, we describe how to estimate the reflectance parameters of the *shadow surface* for a current estimation of the radiance distribution of the scene. In Section 6, we introduce an adaptive sampling framework for efficient approximation of the entire illumination. In Section 7, we show experimental results of the proposed method applied to real images. In Section 8, we present concluding remarks.

[2]In our examples shown in Section 7, we used a modeling tool called the 3D Builder from 3D Construction Company [22] for modeling the shape of an *occluding object* from a *shadow image*. At the same time, the plane of $z = 0$ is defined on the *shadow surface*.

2 Formula for Relating Illumination Radiance with Image Irradiance

In this section, we obtain a formula which relates an illumination distribution of a real scene with the image irradiance of a *shadow image*. The formula will later be used as a basis for estimating the illumination distribution of a real scene and reflectance properties of the *shadow surface*.

2.1 From Illumination Radiance to Scene Irradiance

First, we find a relationship between the illumination distribution of a real scene and the irradiance at a surface point in the scene. To take illumination from all directions into account, let us consider an infinitesimal patch of the extended light source, of a size $\delta\theta_i$ in polar angle and $\delta\phi_i$ in azimuth as shown in Figure 1.

Seen from the center point A, this patch subtends a solid angle $\delta\omega = sin\theta_i\delta\theta_i\delta\phi_i$. Let $L_0(\theta_i, \phi_i)$ be the illumination radiance per unit solid angle coming from the direction (θ_i, ϕ_i); then the radiance from the patch is $L_0(\theta_i, \phi_i)sin\theta_i\delta\theta_i\delta\phi_i$[5], and the total irradiance of the surface point A is

$$E = \int_{-\pi}^{\pi}\int_{0}^{\frac{\pi}{2}} L_0(\theta_i, \phi_i)cos\theta_i sin\theta_i d\theta_i d\phi_i \qquad (1)$$

Then occlusion of the incoming light by the *occluding object* is considered as

$$E = \int_{-\pi}^{\pi}\int_{0}^{\frac{\pi}{2}} L_0(\theta_i, \phi_i)S(\theta_i, \phi_i)cos\theta_i sin\theta_i d\theta_i d\phi_i \qquad (2)$$

where $S(\theta_i, \phi_i)$ are occlusion coefficients; $S(\theta_i, \phi_i) = 0$ if $L_0(\theta_i, \phi_i)$ is occluded by the occluding object; Otherwise $S(\theta_i, \phi_i) = 1$.

2.2 From Scene Irradiance to Scene Radiance

Some of the incoming light at point A is reflected toward the image plane. As a result, point A becomes a secondary light source with scene radiance.

The bidirectional reflectance distribution function (BRDF) $f(\theta_i, \phi_i; \theta_e, \phi_e)$ is defined as a ratio of the radiance of a surface as viewed from the direction (θ_e, ϕ_e) to the irradiance resulting from illumination from the direction (θ_i, ϕ_i). Thus, by integrating the product of the BRDF and the illumination radiance over the entire hemisphere, the scene radiance $Rs(\theta_e, \phi_e)$ viewed from the direction (θ_e, ϕ_e) is computed as

$$Rs(\theta_e, \phi_e) = \int_{-\pi}^{\pi}\int_{0}^{\frac{\pi}{2}} f(\theta_i, \phi_i; \theta_e, \phi_e)L_0(\theta_i, \phi_i) S(\theta_i, \phi_i)cos\theta_i sin\theta_i d\theta_i d\phi_i \qquad (3)$$

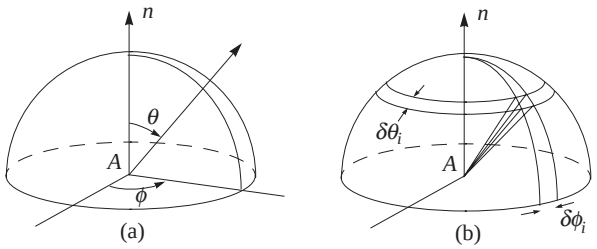

Figure 1. (a) the direction of incident and emitted light rays (b) infinitesimal patch of an extended light source

2.3 From Scene Radiance to Image Irradiance

Finally, the illumination radiance of the scene is related with image irradiance on the image plane. Since what we actually observe is not image irradiance on the image plane, but rather a recorded pixel value in a *shadow image*, it is also necessary to consider the conversion of the image irradiance into a pixel value of a corresponding point in the image. This conversion includes several factors such as D/A and A/D conversions in a CCD camera and a frame grabber.

Other studies concluded that image irradiance was proportional to scene radiance [5]. In our work, we calibrate a linearity of the CCD camera by using a Macbeth color chart with known reflectivity so that the recorded pixel values also become proportional to the scene radiance of the surface. From Equation 3 the pixel value of the *shadow image* $P(\theta_e, \phi_e)$ is thus computed as

$$P(\theta_e, \phi_e) = k \int_{-\pi}^{\pi} \int_{0}^{\frac{\pi}{2}} f(\theta_i, \phi_i; \theta_e, \phi_e) L_0(\theta_i, \phi_i) S(\theta_i, \phi_i) cos\theta_i sin\theta_i d\theta_i d\phi_i \quad (4)$$

where k is a scaling factor between scene radiance and a pixel value. Due to the scaling factor k, we are able to estimate unknown $L_0(\theta_i, \phi_i)(i = 1, 2, .., n)$ up to scale. To obtain the scale factor k, we need to perform photometric calibration between pixel intensity and physical unit ($watt/m^2$) for the irradiance.

2.4 Approximation of Illumination Distribution with Discrete Sampling

In an actual implementation of our method, the illumination distribution is approximated by discrete sampling of radiance over the entire surface of the extended light source. This can be considered as representing the illumination distribution of the scene by using a collection of imaginary directional light sources. As a result, the double integral in Equation 4 is approximated as

$$P(\theta_e, \phi_e) = \sum_{i=0}^{n} f(\theta_i, \phi_i; \theta_e, \phi_e) L(\theta_i, \phi_i) \omega_i S(\theta_i, \phi_i) cos\theta_i \quad (5)$$

where n is the number of sampling directions, $L(\theta_i, \phi_i)$ is the illumination radiance per unit solid angle coming from the direction (θ_i, ϕ_i), which also includes the scaling factor k between scene radiance and a pixel value, and ω_i is a solid angle for the sampling direction (θ_i, ϕ_i).

For instance, node directions of a geodesic dome can be used for uniform sampling of the illumination distribution. By using n nodes of a geodesic dome in a northern hemisphere as a sampling direction, the illumination distribution of the scene is approximated as a collection of directional light sources distributed with an equal solid angle $\omega = 2\pi/n$.

In our method, BRDF $f(\theta_i, \phi_i; \theta_e, \phi_e)$ in Equation 5 is then parameterized using a simplified Torrance-Sparrow model [15, 21]. Using the model, the pixel value of the *shadow image* $P(\theta_e, \phi_e)$, is computed as

$$P(\theta_e, \phi_e) = \sum_{i=0}^{n} (K_d cos\theta_i + K_s \frac{1}{cos\theta_r} e^{\frac{-\gamma(\theta_i, \phi_i)^2}{2\sigma^2}}) S(\theta_i, \phi_i) L(\theta_i, \phi_i) \omega_i \quad (6)$$

where θ_r is the angle between the surface normal and the viewing direction, $\gamma(\theta_i, \phi_i)$ is the angle between the surface normal and the bisector of the light source direction and the viewing direction, K_d and K_s are constants for the diffuse and specular reflection components, and σ is the standard deviation of a facet slope of the Torrance-Sparrow reflection model.

Note that, since each pixel consists of 3 color bands (R, G, and B), each band of radiance $L(\theta_i, \phi_i)$ is also estimated from the corresponding color band of the image separately. Also, based on the dichromatic reflection model, five parameters ($K_{d,R}, K_{d,G}, K_{d,B}, K_s$, and σ) are considered as the reflectance parameters of the *shadow surface*. Accordingly, $L(\theta_i, \phi_i)$ is estimated using K_s, σ, and the corresponding color band of K_d. In this paper, we explain our method by using $L(\theta_i, \phi_i), K_d, K_s$, and σ for the simplicity of our discussion.

3 Basic Steps of the Proposed Method

Based on the formula in Equation 6 which relates the illumination radiance of the scene with the pixel values of the *shadow image*, the illumination radiance distribution of the scene is estimated from image brightness inside shadows as described in the following steps.

1. Initialize the reflectance parameters of the *shadow surface*. Typically, we assume the *shadow surface* to be Lambertian, and the diffuse parameter K_d is set to be the pixel value of the brightest point on the *shadow surface*. The specular parameters are set to be zero $(K_s = 0, \sigma = 0)$. [3]

2. Estimate radiance values $L(\theta_i, \phi_i)$ of imaginary directional light sources which model the illumination distribution of a real scene. By using the reflectance parameters (K_d, K_s, σ) and image brightness inside shadows in the *shadow image*, the radiance distribution $L(\theta_i, \phi_i)$ is computed. (Section 4)

3. Estimate the reflectance parameters of the *shadow surface* (K_d, K_s, σ) from the obtained radiance distribution of the scene $L(\theta_i, \phi_i)$ by using an optimization technique. (Section 5)

4. Estimate the radiance distribution of the scene $L(\theta_i, \phi_i)$ from the obtained reflectance parameters (K_d, K_s, σ). (Section 4)

5. Proceed to the next step if there is no significant change in the estimated values $L(\theta_i, \phi_i), K_d, K_s$, and σ. Otherwise, go back to Step 3. By estimating both the radiance distribution of the scene and the reflectance parameters of the *shadow surface* iteratively, we can obtain the best estimation of those values for a given set of sampling directions of the illumination radiance distribution of the scene.

6. Terminate the estimation process if the obtained illumination radiance distribution approximates the real radiance distribution with sufficient accuracy. Otherwise, proceed to the next step.

7. Increase the sampling directions of the illumination distribution adaptively based on the obtained illumination radiance distribution $L(\theta_i, \phi_i)$ (Section 6). Then go back to Step 2.

We should clarify the assumptions that we made for the proposed method. In our method, it is assumed that light sources in the scene are sufficiently distant from the objects, and thus all light sources project parallel rays onto the object surface. Also, the method does not take into account interreflection between a shadow region and an *occluding object* casting the shadow. We also assume that the *shadow surface* has uniform reflectance properties over the entire surface. Although these assumptions are not exactly true in real situations, we find through experiments that these assumptions have little effect on estimated illumination distribution in most cases.

In the following sections, each step of the proposed method will be explained in more detail.

[3] Note that the initial value of K_d is not so important since there is a scaling factor between the reflectance parameters and illumination radiance values in any case. To fix the scaling factor, we need to perform photometric calibration of our imaging system with a calibration target whose reflectance is given a priori.

4 Estimation of Radiance Distribution based on Reflectance Parameters of Shadow Surface

In this section, we explain how to estimate the radiance distribution of the scene $L(\theta_i, \phi_i)$ for a given set of reflectance parameters (K_d, K_s, σ). In the following sections, we refer $L(\theta_i, \phi_i)$ as to L_i for simplicity.

Using Equation 6 which relates the illumination radiance of the scene with the pixel values of the *shadow image*, illumination radiance is estimated based on the recorded pixel values of the *shadow image*. From Equation 6, a linear equation is obtained for each image pixel of the *shadow image* as

$$a_1 L_1 + a_2 L_2 + a_3 L_3 + \cdots + a_{1n} L_n = P \qquad (7)$$

where L_i $(i = 1, 2, .., n)$ are n unknown illumination radiance specified by n sampling directions of the radiance distribution for the scene. The coefficients $a_i (i = 1, 2, .., n)$ represent $(K_d cos\theta_i + K_s \frac{1}{cos\theta_r} e^{\frac{-\gamma(\theta_i, \phi_i)^2}{2\sigma^2}}) S(\theta_i, \phi_i)$ $(i = 1, 2, .., n)$; we compute θ_i, θ_r, $\gamma(\theta_i, \phi_i)$, and $S(\theta_i, \phi_i)$ based on 3D geometry of the surface point corresponding to the image pixel, the illumination direction, and the shape of the *occluding object*. P is the values of the image pixel $P(\theta_e, \phi_e)$.

If we select a number of pixels, say m pixels, a set of linear equations is obtained as

$$\begin{aligned}
a_{11} L_1 + a_{12} L_2 + a_{13} L_3 + \quad & \cdots + a_{1n} L_n \quad = P_1 \\
a_{21} L_1 + a_{22} L_2 + a_{23} L_3 + \quad & \cdots + a_{2n} L_n \quad = P_2 \\
a_{31} L_1 + a_{32} L_2 + a_{33} L_3 + \quad & \cdots + a_{3n} L_n \quad = P_3 \\
& \cdots \qquad \cdots \\
a_{m1} L_1 + a_{m2} L_2 + a_{m3} L_3 + \quad & \cdots + a_{mn} L_n \quad = P_m
\end{aligned} \qquad (8)$$

Therefore, by selecting a sufficiently large number of image pixels, we are able to solve for a unique solution set of unknown L_i's.

In general, the number of image pixels in shadows is far larger than the number of illumination radiance values to be estimated. Thus we need to select appropriate image pixels for better computational efficiency. In our method, image pixels are selected by considering their coefficients a_i so that the set of linear equations (Equation 8) becomes sufficiently over determined by a smaller number of image pixels.

5 Estimation of Reflectance Parameters of Shadow Surface based on Radiance Distribution

In this section, we describe how to estimate the reflectance parameters of the *shadow surface* (K_d, K_s, σ) by using the estimated radiance distribution of the scene L_i.

Unlike the estimation of the radiance distribution of the scene L_i which can be done by solving a set of linear equations (Equation 8), we estimate the reflectance parameters of the *shadow surface* by minimizing a sum of squared difference between the observed pixel intensities in the *shadow image* and pixel values for the corresponding surface points. Hence the function to be minimized is defined as

$$f = \sum_{j=0}^{m} (P_j{}' - P_j)^2 \tag{9}$$

where $P_j{}'$ is the observed pixel intensities in shadows cast by the *occluding object*, P_j is the pixel value of the corresponding surface points computed by using the given radiance distribution of the scene L_i in Equation 6, m is the number of pixels used for minimization. In our method, the error function in Equation 9 is minimized with respect to the reflectance parameters K_d, K_s, and σ by the Powell method to obtain the best estimation of those reflectance parameters.

6 Adaptive Sampling of Radiance Distribution

If the estimated radiance distribution for a set of sampling directions does not approximate the illumination distribution of the scene with sufficient accuracy, we increase the sampling directions adaptively based on the current estimation of the illumination radiance distribution.

Radiance distribution changes very rapidly around a direct light source such as a fluorescent light. Therefore, the radiance distribution has to be approximated by using a large number of samplings so that the rapid change of radiance distribution around a direct light source is captured. Also, to correctly reproduce soft shadows cast by extended light sources, radiance distribution inside a direct light source has to be sampled densely.

On the other hand, coarse sampling of radiance distribution is enough for an indirect light source such as a wall whose radiance remains small. As a result, the number of sampling directions required for accurately estimating an illumination distribution of a real scene becomes exceedingly large.

To overcome this problem, we increase sampling directions adaptively based on the estimation at the previous iteration, rather than by using a uniform discretization of the overall illumination distribution. In particular, we increase sampling directions around and within direct light sources.

Based on the estimated radiance distribution L_i for the sampling directions at the previous step, additional sampling directions are determined as follows.

Suppose three sampling directions with radiance values L_1, L_2, and L_3 are placed to form a triangle M_1 as illustrated in Figure 2. To determine whether a new sampling direction needs to be added between L_1 and L_2 or not, we consider the following cost function.

$$U(L_1, L_2) = diff(L_1, L_2) + \alpha min(L_1, L_2) angle(L_1, L_2) \tag{10}$$

where $diff(L_1, L_2)$ is the radiance difference between L_1 and L_2, $min(L_1, L_2)$ gives the smaller radiance of L_1 and L_2, $angle(L_1, L_2)$ is the angle between directions to L_1 and L_2, and α is a manually specified parameter which determines the relative weights of those two factors. The first term is required to capture the rapid change of radiance distribution around direct light sources, while the second term leads to fine sampling of the radiance distribution inside direct light sources. The additional term $angle(L_1, L_2)$ is used for avoiding unnecessarily dense sampling inside direct light sources. In our experiments, α is set to 0.5.

If the cost U is large, a new sampling direction is added between L_1 and L_2. In our experiments, we computed the cost function values U for all pairs of neighboring sampling directions, then added additional sampling directions for the first 50% of all the pairs in order of the cost function values U.

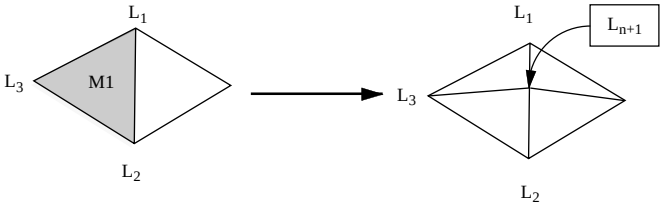

Figure 2. Subdivision of sampling directions

7 Experimental Results

We have tested the proposed method by using real images taken in both indoor and outdoor environments.

An image with an *occluding object*, i.e., *shadow image*, was taken under usual illumination environment in our office, including direct light sources such as fluorescent lamps, as well as indirect illumination such as reflections from a ceiling and a wall. The input image is shown in Figure 3 (a).

First, the shape of the *occluding object* and the camera parameters of the input image were obtained by using a

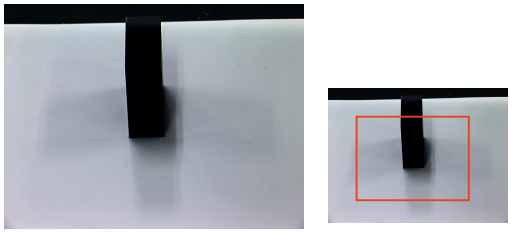

Figure 3. Input image : (a) *shadow image* taken in an indoor scene (b) the region where synthesized images with the estimated radiance distribution and reflectance parameters are superimposed in Figure 4

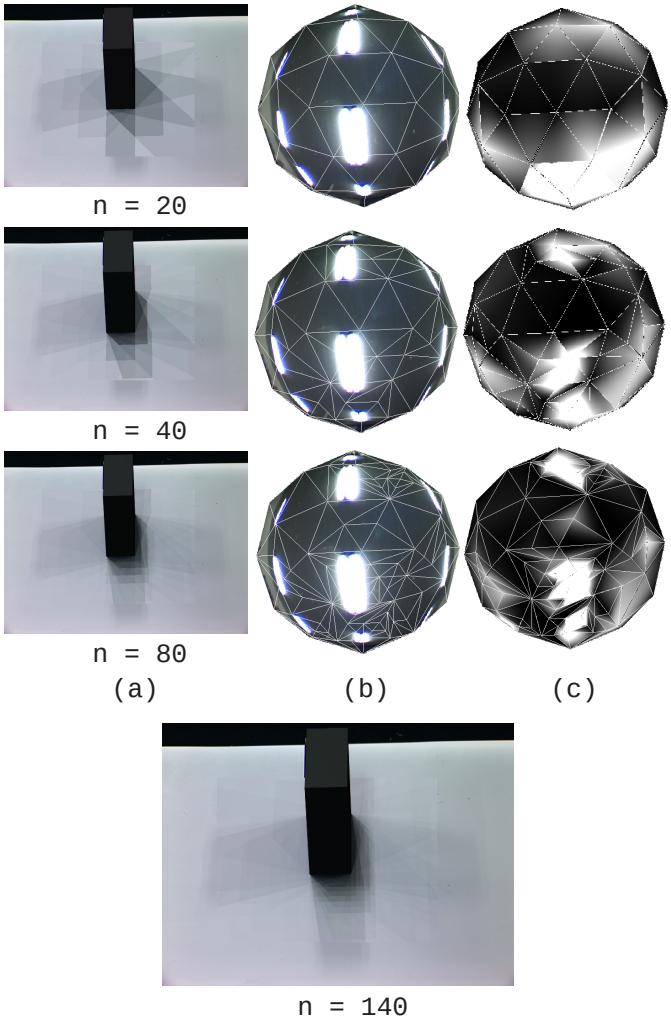

Figure 4. Adaptive refinement of illumination distribution estimation: (a) synthesized images with the estimated radiance distribution and reflectance parameters (b) adaptive refinement of sampling directions with a ground truth of an omni-directional image of the scene (c) the estimated radiance values visualized for comparison with the ground truth

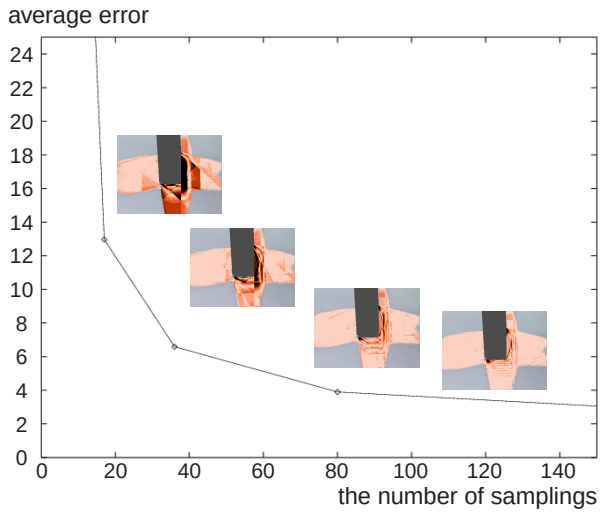

Figure 5. Error Analysis

photo-modeling tool [22]. Then, an illumination distribution of the scene was estimated using the image irradiance inside shadows in the *shadow image* as explained in Section 3. Starting from a small number of uniform sampling directions of the illumination distribution, the estimation of the radiance distribution of the scene was iteratively refined as described in Section 6. At the same time, the reflectance parameters (K_d, K_s, and σ) of the *shadow surface* were estimated as explained in Section 5.

Then an appearance of the *shadow surface* around the *occluding object* was synthesized by using the estimated radiance distribution of the scene and the estimated reflectance parameters of the *shadow surface*. To demonstrate how well the estimated radiance distribution and the reflectance parameters could represent the scene, we replaced the region inside the red rectangle in Figure 3 (b) with the synthesized appearances. The left column in Figure 4 shows the results synthesized by the estimated radiance distribution and the estimated reflectance parameters of the *shadow surface*. The number of sampling directions of the radiance distribution used for the estimation is shown under the resulting images.

We found through our experiments that, the larger number of sampling directions we used, the more the shadows of the synthetic object resembled those of the *occluding object* in the *shadow image*. Especially in the case of 140 sampling directions, we can see hardly any distinct boundaries in the shadows, and the synthesized shadow of the *occluding object* matches the real one in the input image very well: this shows that the estimated illumination distribution gives a good presentation of that of the real scene.

To see how well the adaptive sampling of radiance distribution works for real images, we took an omni-directional

image of the office scene as a ground truth. The middle column of Figure 4 shows the omni-directional image of the scene taken by placing a camera with a fisheye lens looking upward on the *shadow surface* in Figure 3 (a). The omni-directional image shows both direct light sources, i.e., fluorescent lamps in our office, and indirect light sources such as a ceiling and walls. The right column of Figure 4 shows the estimated radiance values visualized for comparison with the ground truth. In those images in Figure 4 (b) and (c), we can see that sampling directions of the radiance distribution were nicely added only around the direct light sources at each step by the proposed adaptive sampling framework, starting from the coarse sampling directions at the top row.

Figure 5 numerically shows the improvement of the accuracy by adaptive refinement of sampling directions and the estimation of reflectance properties of the *shadow surface*. The vertical axis represents average error in pixel values inside the synthesized images in the region shown in Figure 3 (b) compared with that in the input image Figure 3 (a). Here, the initial average pixel values of shadow regions in the *shadow image* are set to 100 %. The horizontal axis represents the number of sampling directions used for the estimation. From the plot in the figure, we can clearly see that the accuracy improves rapidly as we adaptively increase sampling directions of the radiance distribution. Also the small pictures at the bottom show error distributions inside the region. Darker color represents larger error in a pixel value in the shadow regions compared with the real shadows of the *occluding object* in the *shadow image*.

To confirm the merit of the adaptive sampling framework and the estimation of the reflectance parameters of the *shadow surface*, we also estimated the illumination radiance distribution with uniform sampling and fixed reflectance parameters. In that case, even 300 uniformly sampled directions could not achieve the same level of accuracy as the estimation result obtained by 80 sampling directions with the method proposed in this work.

Figure 6 (a) shows another example image taken outside the entrance lobby of our building in the late afternoon. In this image, we used the rectangular pole with two colors as an *occluding object* casting shadows. In the same way as the previous example, the shape of the *occluding object* and the camera parameters of the input image were obtained by using a photo-modeling tool. Then, an illumination distribution of the scene was estimated using the image irradiance inside shadows in the input image as explained in Section 3.

Then an appearance of the *shadow surface* around the *occluding object*, illustrated with a red rectangle in Figure 7 (b), was synthesized by using the estimated radiance distribution of the scene and the estimated reflectance parameters of the *shadow surface* [18]. Figure 7 shows the resulting images by our method. Although the grid pattern on the *shadow surface* is missing in those synthesized images due to the assumption of uniform reflectance on the *shadow image*, the appearance of the shadow around the *occluding objects* is virtually indistinguishable in the case of 140 sampling directions. This shows that the estimated illumination distribution gives a good representation of the characteristics of the real scene.

Figure 6. Input image : (a) *shadow image* taken in an outdoor scene (b) the region where synthesized images with the estimated radiance distribution and reflectance parameters are superimposed in Figure 7

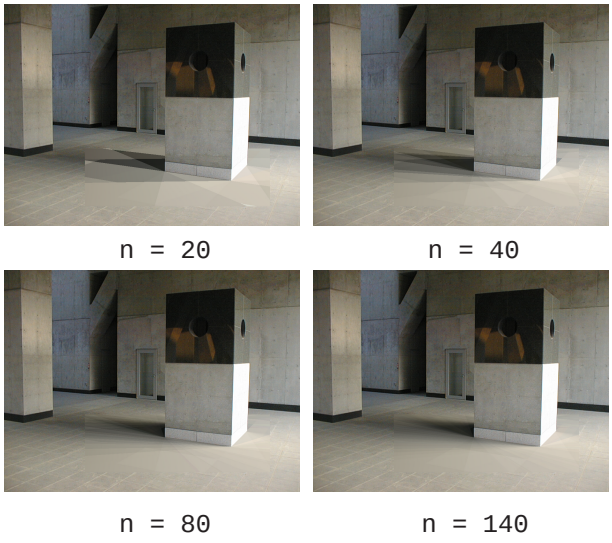

Figure 7. Adaptive refinement of illumination distribution estimation: synthesized images with the estimated radiance distribution and reflectance parameters

8 Conclusions

In this paper, we have proposed a new method for estimating an illumination distribution of a real scene from a radiance distribution inside shadows cast by a real object

of known shape onto other object surfaces of known shape and known reflectance. By using the occlusion information of the incoming light, we were able to estimate an illumination distribution of a real scene reliably, even for the images taken in a complex illumination environment.

In particular, the proposed method has been significantly extended from our previous approach in two main aspects. First, we combine the illumination analysis with an estimation of the reflectance properties of a shadow surface. As a consequence, the proposed method becomes applicable to the case where reflectance properties of a surface are not known. Second, we propose an adaptive sampling framework for efficient estimation of illumination distribution. Rather than using a uniform discretization of the overall illumination distribution, we adaptively increase the sampling directions of the illumination distribution based on the estimation at the previous iteration. Using this adaptive sampling framework, we can avoid unnecessarily dense sampling of the illumination and estimate the entire illumination distribution more efficiently with a smaller number of sampling directions of the illumination distribution.

To demonstrate the effectiveness of the proposed method, we have successfully tested our method by using sets of real images taken in our office with different surface materials of shadow regions.

Acknowledgments

This research was supported by the Ministry of Education, Science, Sports and Culture grant-in-Aid for Creative Basis Research 09NP1401.

References

[1] R. Baribeau, M. Rioux, and G. Godin, "Color Reflectance Modeling Using a Polychromatic Laser Range Sensor," *IEEE Trans. PAMI*, vol. 14, no. 2, pp. 263-269, 1992.

[2] J. Bouguet and P. Perona, "3D Photography on Your Desk," *Proc. IEEE Intl. Conference on Computer Vision 98*, pp.43-50, 1998.

[3] A. Fournier, A. Gunawan and C. Romanzin, "Common Illumination between Real and Computer Generated Scenes,"*Proc. Graphics Interface '93*, pp.254-262, 1993.

[4] B. K. P. Horn,"Understanding Image Intensities," *Artificial Intelligence, 8(2)*, pp.201-231, 1977.

[5] B. K. P. Horn, *Robot Vision*, The MIT Press, Cambridge, MA., 1986.

[6] B. K. P. Horn, "Obtaining Shape from Shading Information," *The psychology of Computer Vision*, McGraw-Hill Book Co., New York, N.Y., 1975.

[7] B. K. P. Horn and M. J. Brooks, "The Variational Approach to Shape from Shading," *Computer Vision, Graphics, and Image Processing*, 33(2), pp.174-208, 1986.

[8] K. Ikeuchi and B. K. P. Horn, "Numerical Shape from Shading and Occluding Boundaries," *Artificial Intelligence 17(1-3)*, pp.141-184, 1981.

[9] K. Ikeuchi and K. Sato, "Determining Reflectance using Range and Brightness Images," *Proc. IEEE Intl. Conference on Computer Vision 90*, pp.12-20, 1990.

[10] J. R. Kender and E. M. Smith, "Shape from Darkness: Deriving Surface Information from Dynamic Shadows," *Proc. IEEE Intl. Conference on Computer Vision 87*, pp.539-546, 1987.

[11] G. Kay and T. Caelli, "Estimating the Parameters of an Illumination Model using Photometric Stereo,"*Graphical Models and Image Processing*, vol. 57, no. 5, pp. 365-388, 1995.

[12] J. Lu and J. Little, "Reflectance Function Estimation and Shape Recovery from Image Sequence of a Rotating Object,"*Proc. IEEE Intl. Conference on Computer Vision '95*, pp. 80-86, 1995.

[13] A. K. Markworth, "On the Interpretation of Drawings as Three-Dimensional Scenes," *PhD thesis, University of Sussex*, 1974.

[14] S. R. Marschner and D. P. Greenberg, "Inverse Lighting for Photography," *Proc. IS&T/SID Fifth Color Imaging Conference*, pp.262-265, 1997.

[15] S. K. Nayar, K. Ikeuchi, and T. Kanade, "Surface reflection: physical and geometrical perspectives," *IEEE Trans. PAMI*, vol. 13, no. 7, pp. 611-634, 1991.

[16] A. P. Pentland, "linear Shape From Shading," *Intl. J. Computer Vision*, 4(2), pp153-162, 1990.

[17] Y. Sato, M. D. Wheeler, and K. Ikeuchi, "Object shape and reflectance modeling from observation," *Proc. SIGGRAPH 97*, pp. 379-387, 1997.

[18] I. Sato, Y. Sato, and K. Ikeuchi, "Acquiring a Radiance Distribution to Superimpose Virtual Objects onto a Real Scene", *IEEE Trans. Visualization and Computer Graphics*, vol. 5, no. 1, pp. 1-12, 1999.

[19] I. Sato, Y. Sato, and K. Ikeuchi, "Illumination from Shadows", *Proc. IEEE Conference on Computer Vision and Pattern Recognition 99*, pp.306-312, 1999.

[20] S. A. Shafer and T. Kanade, "Using Shadows in Finding Surface Orientations," *Computer Vision, Graphics, and Image Processing*, 22(1), pp. 145-176, 1983.

[21] K. E. Torrance and E. M. Sparrow, "Theory for off-specular reflection from roughened surface," *J. Optical Society of America*, vol.57, pp.1105-1114, 1967.

[22] 3D Construction Company, http://www.3dcomstruction.com